

# Post-Training Quantization for Object Detection

Lin Niu <sup>\*, $\diamond$</sup>  Jiawei Liu <sup>\*, $\diamond$</sup>  Xinggang Wang Wenyu Liu<sup>†</sup>  
School of EIC, Huazhong University of Science & Technology, Wuhan, China  
{linniu, jiaweiliu, xgwang, liuwy}@hust.edu.cn

Dawei Yang Zhihang Yuan<sup>†</sup>  
Houmo AI, Nanjing, China  
{hahnyuan, dawei.yang}@houmo.ai

## Abstract

*Efficient inference for object detection networks is a major challenge on edge devices. Post-Training Quantization (PTQ), which transforms a full-precision model into low bit-width directly, is an effective and convenient approach to reduce model inference complexity. But it suffers severe accuracy drop when applied to complex tasks such as object detection. PTQ optimizes the quantization parameters by different metrics to minimize the perturbation of quantization. The  $p$ -norm distance of feature maps before and after quantization,  $L_p$ , is widely used as the metric to evaluate perturbation. For the specialty of object detection network, we observe that the parameter  $p$  in  $L_p$  metric will significantly influence its quantization performance. We indicate that using a fixed hyper-parameter  $p$  does not achieve optimal quantization performance. To mitigate this problem, we propose a framework, DetPTQ, to assign different  $p$  values for quantizing different layers using an Object Detection Output Loss (ODOL), which represents the task loss of object detection. DetPTQ employs the ODOL-based adaptive  $L_p$  metric to select the optimal quantization parameters. Experiments show that our DetPTQ outperforms the state-of-the-art PTQ methods by a significant margin on both 2D and 3D object detectors. For example, we achieve 31.1/31.7(quantization/full-precision) mAP on RetinaNet-ResNet18 with 4-bit weight and 4-bit activation.*

## 1. Introduction

Benefiting from the incredible power of deep learning, object detection networks [29, 22] have achieved eye-popping performance. However, a large number of parameters and storage requirements present challenges for real-

time inference when deployed on edge devices in the real world such as smartphones and electric cars. It is necessary to reduce the memory footprint and computational cost for efficient inference.

There are various methods for compressing Convolutional Neural Networks (CNNs) to improve inference efficiency, such as pruning [13], quantization [10], and knowledge distillation [11]. Among these methods, quantization is particularly promising as it converts full-precision (FP) values to integer grids, reducing computational burden. Quantization can be further divided into two types: Quantization-Aware Training (QAT)[8] and Post-Training Quantization (PTQ)[25]. Many researchers have retrained object detection networks using labeled training datasets for quantization (i.e., QAT) and achieved great performance. However, QAT can be hindered by the unavailability of labeled datasets due to privacy concerns and the time-consuming training process. PTQ, on the other hand, aims to quantize pre-trained models without retraining, only requiring a small un-labeled calibration dataset. It is popular for deployment in real-world applications.

Current PTQ methods mainly focus on image classification, with little exploration into their application in object detection. Object detection networks not only classify multiple objects but also regress the location offsets of bounding boxes. These networks have complex architectures, often containing multi-level and multi-dimensional outputs, as opposed to a single vector output in classification networks. These multi-level outputs detect objects of various scales. We observe that different detection levels have different sensitivities to quantization perturbation. When quantizing object detection networks, it suffers a significant performance drop, especially in extremely low-bit settings.

The goal of quantization is to find the optimal quantization parameters that allow the quantized network to achieve the best task performance (minimizing the task loss or maximizing metrics such as mAP [23]). However, because la-

<sup>\*</sup> Equal contribution.  <sup>$\diamond$</sup>  This work was done when Lin Niu and Jiawei Liu were interns at Houmo AI. <sup>†</sup> Corresponding authors.

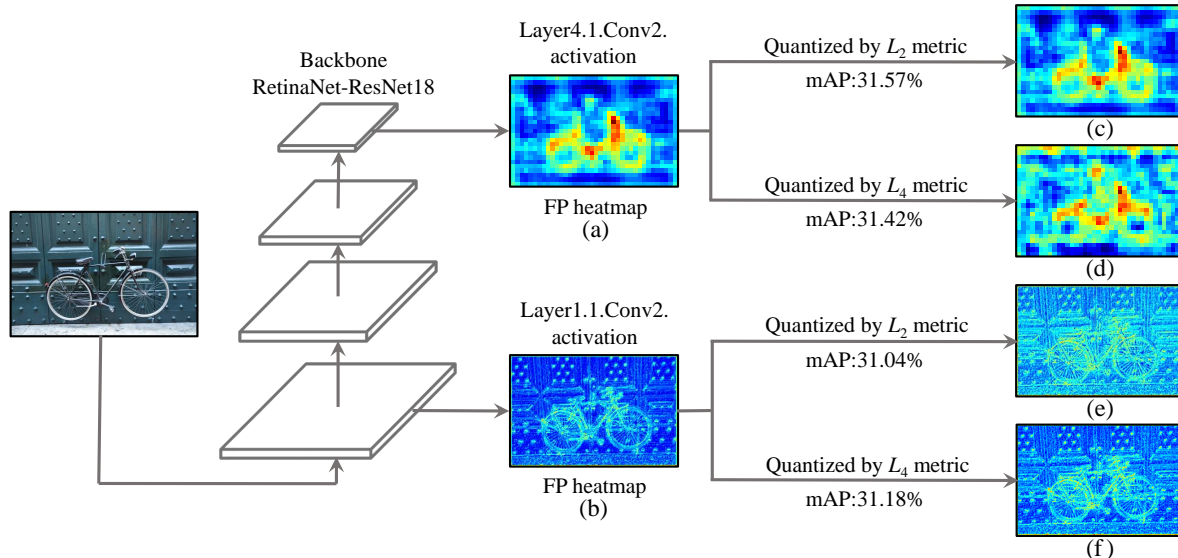


Figure 1: Visualization of the 4-bit PTQ on different activation layers using different  $L_p$  metrics in an object detection network (RetinaNet-ResNet18). All the mAP results are reported on the COCO validation set when quantizing only one activation layer of the network. (c), (d), (e) and (f) show the heatmap of the quantized activation.

beled data is not available in PTQ, the network’s task performance cannot be directly evaluated. To approximate the task loss, previous PTQ methods [25, 20, 32] often optimize the quantization parameters layer-wise or block-wise to minimize the reconstruction loss for the output of the intermediate layers or blocks, known as local quantization reconstruction. They hypothesize that the block-wise (or layer-wise) optimization is mutual-independent and lack attention to the final task output. Those methods use a fixed metric to evaluate (such as  $L_2$  loss) the intermediate feature maps before and after quantization. In this paper, we argue that *using a fixed metric without considering its sensitivity to task performance will negatively impact the quantization performance.*

In this paper, we find that the parameter  $p$  in the  $L_p$  metric has a significant impact on the quantization of object detection networks. We investigate the influence of different  $L_p$  metrics on quantization parameters which generated by local quantization reconstruction. We also visualize the quantized feature maps with different  $L_p$  metrics. Taking Figure 1 as an example, we observe that setting  $L_2$  as quantization metric brings better task performance for the upper level feature map, while setting  $L_4$  metric is more beneficial to the lower level feature map. This phenomenon is especially obvious in detection networks. We conclude that *different levels of feature maps require different  $L_p$  metrics to achieve better detection performance.*

To determine the optimal  $p$  values for different levels of features, we propose DetPTQ to select the  $p$  value that makes the local  $L_p$  loss approximate to the final task loss.

Because labeled data is not available in PTQ, we propose the Object Detection Output Loss (ODOL) which can represent the curve change of the task performance loss when quantizing the network. DetPTQ chooses the  $p$  value that makes the  $L_p$  loss approximate to the ODOL. To evaluate our method, we experiment on various architectures, including the one-stage 2D detection network RetinaNet [22], the two-stage 2D detection network Faster RCNN [29], and the point cloud 3D detection network PointPillar [18]. Our work makes the following contributions:

1. We indicate that local quantization reconstruction requires an adaptive loss metric for PTQ on object detection networks.
2. We propose a PTQ framework, DetPTQ, that assigns different  $L_p$  metric to quantize the different layers. We propose the ODOL, an approximation of the task loss, to model the global information.
3. Experiments on 2D and 3D object detectors show that DetPTQ outperforms the state-of-the-art PTQ methods. For example, DetPTQ achieves less than 1% mAP drop with 4-bit PTQ on all of the ResNet-based networks for the first time.

## 2. Related Work

### 2.1. Quantization-aware Training (QAT)

QAT [17, 5, 8] uses the entire training datasets to optimize the network for quantization. The quantization function quantizes tensors in forward-propagation, which has

zero-gradient almost everywhere. QAT methods utilize the Straight Through Estimator (STE) [2] to avoid the zero-gradient problem. Recently, object detection quantization has attracted extensive attention for on-device deployment. [16] constrains the bitwidth of objection detection quantization to 8-bit (W8A8), and achieves good results on COCO dataset [23]. FQN [19] quantizes RetinaNet [22] and FasterRCNN [29] to 4-bit for the first time and demonstrates usable performance. AQD [4] pushes the limits of bit-width in object detection network quantization down to 2-bit. Although QAT methods achieve promising results in object detection, extensive training cost and the requirement of labeled datasets prevent its real-world deployment.

## 2.2. Post-training Quantization (PTQ)

Compared with QAT, PTQ [1, 33, 14] plays an important role in fast network deployment. AdaRound [25] minimizes the  $L_2$  loss layer-wisely to optimize a rounding scheme and scale factors. Brecq [20] introduces block reconstruction to improve AdaRound. QDrop [32] shows decent performances at 2-bit by randomly dropping quantized activation during local reconstruction. PD-Quant [24] proposes the prediction difference loss (PD-loss) as an approximation of the task loss. PD-Quant only explores the metric to classification tasks and requires forward propagation to calculate PD-loss too many times. We explore the object-detection-based prediction difference loss. As the computation cost of object detection is much higher than classification, the adaptive local  $L_p$  loss in our DetPTQ can greatly reduce the quantization overhead.

Previous works explore the influence of metrics to measure the difference relative to the full-precision for PTQ. LAPQ [27] find that scale factors from different  $L_p$  metrics will cause different quantization errors. It adopts the Powell Algorithm to jointly optimize scale factors from different  $L_p$  metrics. PTQ4ViT [36] proposes to utilize a Hessian-guided metric to evaluate different scale factors for vision transformer. RAPQ [34] shows a theory that  $p$  value is positively correlated with the sensitivity of the  $L_p$  loss value to outliers. It takes the variance information from BN [15] to define a BN-based  $L_p$  loss. In our method, we use the global task information (i.e., ODOL) to set the  $p$  value.

Object detection networks often generate multi-level outputs or carry out feature fusion by FPN [21] to detect objects of different scales. Many PTQ methods such as Brecq and QDrop have successfully extended to objection detection networks but they do not consider the characteristics of object detection networks. They use fixed loss in local reconstruction, which is sub-optimal. Because different levels have different sensitivities, we propose an adaptive loss in local reconstruction.

## 3. Preliminaries

The quantization function transforms a float-point value  $x$  to an integer value  $\tilde{x}$ , and  $x^q$  represents the dequantized float value with some error from  $x$ :

$$\tilde{x} = clip(\lfloor \frac{x}{s} \rceil + z, n, m) \quad (1)$$

$$x^q = (\tilde{x} - z) \cdot s \quad (2)$$

where  $\lfloor \cdot \rceil$  means that the input  $\frac{x}{s}$  is rounded to the nearest integers (i.e., rounding-to-nearest), which causes the rounding error  $\Delta r$ .  $clip(\cdot)$  clips the values that lie outside of integer range  $[n, m]$ , which causes the clipping error  $\Delta c$ .  $\tilde{x}$  denotes the integer value,  $z$  is zero-point and  $s$  denotes the quantization scale factor. The total perturbation of quantization is  $\Delta p = \Delta c + \Delta r = x - x^q$ .

PTQ searches for the optimal quantization parameters by solving the problem of minimizing the local reconstruction loss:

$$\arg \min_s \|O - O^q\|_2 \quad (3)$$

where  $O$  denotes a FP tensor.  $O^q$  is the quantized tensor.  $\|\cdot\|_2$  denotes the  $L_2$  loss (MSE). For simplicity, we denote all of the quantization parameters with  $s$ . Previous PTQ methods [1, 6] sequentially search the quantization parameters  $s$  to minimize the local reconstruction loss layer-by-layer or block-by-block without any training or fine-tuning. This is referred to as the **simple PTQ method**.

Recently, some **advanced PTQ methods** have been proposed, such as AdaRound, BRECQ and QDrop, which reconstruct the weight for better quantization. They bring an extra variable  $v$  to each weight  $w$  and optimize the variable to minimize the local reconstruction loss of the output of a block. The quantization function and the optimization are formulated as:

$$\tilde{w} = clip(\lfloor \frac{w+v}{s} \rceil + z, n, m), w^q = (\tilde{w} - z) \cdot s \quad (4)$$

$$\arg \min_{V,s} \|O - O^q\|_2 \quad (5)$$

where  $V$  is all of the extra variables in a block. Our method is orthogonal to the selection of simple PTQ and advanced PTQ, so we denote  $s$  as all of the quantization parameters including  $V$  for simplicity.

To analyze the influence of the metric for quantization perturbation, we replace the  $L_2$  loss with the  $L_p$  loss (MSE can be regarded as a special case of  $p = 2$ ). The local reconstruction loss is changed to:

$$\|O - O^q\|_p = (\sum_i \|O_i - O_i^q\|_p)^{1/p} \quad (6)$$

RAPQ [34] has demonstrated that the  $p$  value of the  $L_p$  loss is positively correlated with the clipped range. For object

Metric	Layer1.1.Conv2		Layer4.1.Conv2	
	$s$	$\mathcal{L}_{perf}$	$s$	$\mathcal{L}_{perf}$
Min-Max	0.3472	6.00	0.5068	0.30
$L_1$	0.1076	2.14	0.2246	3.17
$L_2$	0.1885	0.63	<b>0.3462</b>	<b>0.10</b>
$L_3$	<b>0.2102</b>	<b>0.45</b>	0.4273	0.21
$L_4$	0.2695	0.49	0.4982	0.25

Table 1: Comparison of performance loss among different metrics for 4-bit quantization of RetinaNet-Resnet18. We only optimize the scale factor  $s$  of one layer’s output activation to minimize the local reconstruction error evaluated by  $L_p$  metrics. Min-Max is to set the scale factor  $s$  that covers all of the activation distribution.

detection networks, we also find that a larger  $p$  for  $L_p$  metric leads to a larger scale factor, and vice versa. Next, we will deeply explore the influence of different  $p$  values.

## 4. Method

### 4.1. Influence of Different $p$ Values

The goal of quantization algorithm is to find the optimal quantization parameters to minimize the performance loss caused by the quantization perturbation. PTQ methods usually use MSE ( $L_2$ ) to measure the difference before and after quantization to evaluate the performance loss. Since mean Average Precision (mAP) is the main evaluation metric for object detection task, the performance loss can be defined as

$$\mathcal{L}_{perf} = mAP^{fp} - mAP^q \quad (7)$$

where  $mAP^{fp}$  denotes the performance of the FP network on validation set, which is a constant value for a pre-trained model.  $mAP^q$  is the performance of the quantized network.

To investigate the influence of different  $p$  values of  $L_p$  metric on different layers, we compare the results of performance loss when quantizing only one layer of the network. In Table 1, we observe that the quantization parameters  $s$  are quite different using different  $p$ . There are also significant differences in performance losses. For Layer1.1.Conv2, we observe that the scale factor from  $L_3$  has minimal performance loss (0.49), while the scale factor chosen by  $L_2$  (MSE) metric is sub-optimal (performance loss is 0.66). As a hyper-parameter of  $L_p$  metric, the best  $p$  value is different for different layers. In this example,  $L_2$  is the best for Layer4.1.Conv2, while  $L_3$  is the best for Layer1.1.Conv2. Using a fixed  $L_p$  metric does not bring to the optimal quantization parameters.  $p$  values need to be adjusted for different layers or blocks.

The visualization plot of feature maps in Figure 1 demonstrates the influence of different  $p$  values. The output activation from Layer1.1.Conv2 is to detect small tar-

gets. From the heatmap (b) using  $L_2$ , we can observe that the large activation values are clipped to the same value as small activations, causing the detector cannot distinguish the small objects. A larger  $p$  is better to get a larger scale factor  $s$ , reducing the clipping error on large activations. From the heatmap (b) using  $L_4$ , the small objects can be distinguished. The results also show quantizing it using  $L_4$  (31.18% mAP) is better than  $L_2$  (31.04% mAP). Regarding the high-level activation Layer4.1.Conv2, it detects big targets and is more sensitive to global semantic information. The heatmap (c) illustrates that clipping large activation values by  $L_4$  metric does not significantly affect the detection of big targets. It is more inclined to use a small  $p$  value for the  $L_p$  metric to achieve a higher mAP. We conclude that different level activations call for different  $L_p$  metrics to achieve accurate detection performance for PTQ. Choosing the right  $L_p$  metric to search for the optimal quantization parameters that lead to optimal performance loss is the key issue addressed in the following section.

### 4.2. Object Detection Output Loss (ODOL)

It is a challenge to select the  $p$  in  $L_p$  metric for local quantization reconstruction. Note that the goal of quantization algorithm is to find the optimal quantization parameters to minimize the performance loss  $\mathcal{L}_{perf}$ . Because the  $p$  value becomes a variable, the formulation of local reconstruction optimization is:

$$\arg \min_p \mathcal{L}_{perf}(s_p^*) \quad (8)$$

$$s_p^* = \arg \min_s \|O - O^q\|_p \quad (9)$$

where  $s_p^*$  is the optimal quantization parameters given  $p$  for local reconstruction and  $\mathcal{L}_{perf}(s_p^*)$  is the performance loss with the quantized network using  $s_p^*$ . We denote  $s_{ideal}^*$  as the ideal quantization scaling factor, which leads to the lowest performance loss  $\mathcal{L}_{perf}$  assuming we have the labeled data. However, there is no label for PTQ’s calibration data to calculate the  $mAP$  and the  $\mathcal{L}_{perf}$ . Next, we will propose the Object Detection Output Loss (ODOL) that measures the output difference between the quantized network and FP network as an approximation to  $\mathcal{L}_{perf}$ . We expect that the scale factor, which is optimized by the function, is consistent with  $s_{ideal}^*$ .

The output of object detection networks usually contains two parts: the score for classification and the offset for regression. For classification part, we calculate the distance of probabilities predicted by FP network and quantized network for **all boxes**, which is denoted as class loss  $\mathcal{L}_{cls}$ . For regression part, we calculate the coordinate distance of the boxes predicted by FP network and quantized network for **positive boxes**, which is denoted as localization loss  $\mathcal{L}_{loc}$ . The function expression of ODOL is formulated as follow-

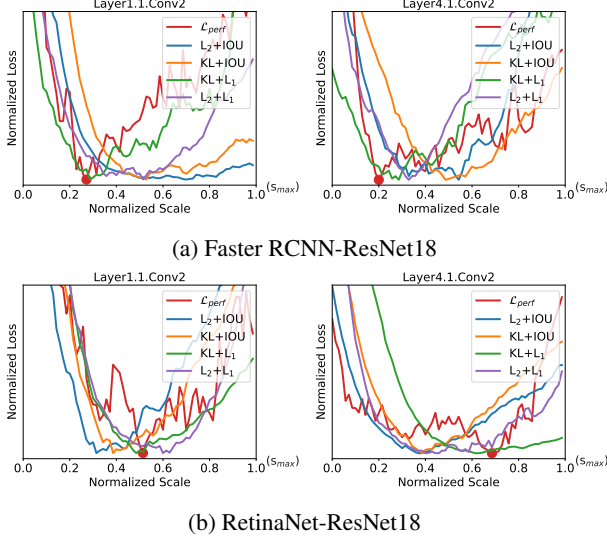


Figure 2: Quantization scale-loss curves with different loss functions. The scaling factor  $s_{max}$  is calculated by Min-Max quantization and then normalized to 1.0. The loss values (y-axis) are normalized for comparison.

ing:

$$\mathcal{L}_{ODOL} = \frac{1}{N} \sum_{i=1}^N (\mathcal{L}_{cls,i} + \alpha \mathcal{L}_{loc,i} I_{pos,i}) \quad (10)$$

$$\mathcal{L}_{cls,i} = MSE(c_i, c_i^q) \quad or \quad KL(c_i, c_i^q) \quad (11)$$

$$\mathcal{L}_{loc,i} = L_1(l, l^q) \quad or \quad IOU(l, l^q) \quad (12)$$

where the  $I_{pos,i}$  is the indicator of whether the  $i$ -th box is a positive box.  $N$  denotes the number of anchors.  $\alpha$  is a balanced weight.  $c$  and  $l$  refer to FP output of scores and coordinates, while  $c^q$  and  $l^q$  are the output of scores and coordinates from the quantized network.

We explore various functions for ODOL. We attempt  $L_2$  distance and KL distance to measure the classification difference  $\mathcal{L}_{cls}$ . For localization loss  $\mathcal{L}_{loc}$ , we attempt  $L_1$  distance and IOU loss [35] to measure the distance of coordinate between the FP boxes and quantized boxes. To evaluate different loss functions, we compare different scale-loss curves in Figure 2. The red line is the performance loss, and the ideal scale  $s_{ideal}^*$  is located in the red point. We can observe that the scale factor optimized by ODOL with KL+ $L_1$  (green line) is close to  $s_{ideal}^*$ . Taking an instance, when quantizing the activation of Retinanet-resnet18 Layer1.1.Conv2,  $s_{ideal}^*$  is around  $0.48 \times s_{max}$ , which is almost the same as ODOL with KL+ $L_1$  optimized. We will show more experiment results for the different combinations of ODOL

We filter all boxes by a threshold on the score from FP network and select the top 500 boxes. Then we perform NMS [28] on those  $k$  boxes to produce positive boxes and indicator  $I_{pos,i}$ . We decode the predicted offset to get the real coordinate for  $l$  and  $l^q$ .

in Section 5.3. According to the experimental findings, we choose KL as the  $\mathcal{L}_{cls}$  and  $L_1$  as the  $\mathcal{L}_{loc}$  as an approximation of  $\mathcal{L}_{perf}$ .

---

### Algorithm 1 Network quantization using DetPTQ

---

**Input:** calibration dataset  $X^1$  and a network with  $L$  blocks.

**Output:** quantization parameters of both activation and weight in network

- 1: input  $X^1$  to FP network to get the FP output;
  - 2: **for**  $B_l = \{B_i | i = 1, 2, \dots, L\}$  **do**
  - 3:   Initialize a list  $D$ ;
  - 4:   Input  $X^l$  from quantized block  $B_{l-1}$  to FP block  $B_l$ ;
  - 5:   **for**  $P = \{p_i | i = 1, 2, \dots, k\}$  **do**
  - 6:     Optimize only activation quantization parameters to minimize Eq 14 in block  $B_l$  to get  $s_p^*$ ;
  - 7:     Quantize activations in  $B_l$  to get  $O^q$ ;
  - 8:     Input  $O^q$  to the following FP network to get output of partial-quantized network;
  - 9:     Calculate  $\mathcal{L}_{ODOL}(s_p^*)$  using Eq 10;
  - 10:     Append  $\mathcal{L}_{ODOL}(s_p^*)$  to list  $D$ ;
  - 11:   **end for**
  - 12:    $index \leftarrow \text{argmin}(D)$ ;
  - 13:    $p^* \leftarrow P[index]$ ;
  - 14:   Optimize quantization parameters for both activation and weight to minimize Eq 14 using  $p^*$  in block  $B_l$ ;
  - 15:   Quantize weights and activations in  $B_l$  to get  $O^q$ ;
  - 16:    $O^q$  as the input  $X^{l+1}$  to next FP block  $B_{l+1}$ ;
  - 17: **end for**
- 

### 4.3. DetPTQ Framework

One intuition is that we can use ODOL as a metric to directly optimize the quantization parameters to minimize the distance for the intermediate layer’s activation before and after quantization, just as PD-Quant [24] and NWQ [31] do. However the computation cost of object detection is very large. Repeated forward propagation to calculate ODOL is not realistic. In the section above, we observe that the parameter  $p$  in  $L_p$  metric has a significant influence on quantization. And we propose ODOL as an approximation of performance loss to determine  $p$  value for  $L_p$  metric. In this case, ODOL is computed as many times as the number of candidate  $p$  values. The local quantization reconstruction using ODOL can be formulated as:

$$\arg \min_p \mathcal{L}_{ODOL}(s_p^*) \quad (13)$$

$$s_p^* = \arg \min_s \|O - O^q\|_p \quad (14)$$

Next, we will propose our PTQ framework, DetPTQ. The same as previous methods, we quantize blocks in sequential order so that the perturbation accumulated in earlier blocks can be made up. When quantizing the  $l_{th}$  Block ( $B_l$ ), the

Method	Bits(W/A)	Faster RCNN			RetinaNet		
		ResNet-18	ResNet-50	MobileNetV2	ResNet-18	ResNet-50	MobileNetV2
FP	32/32	34.23	38.46	29.91	31.67	37.38	28.40
MSE	4/8	31.02	35.35	19.02	28.64	34.88	9.85
Cosine	4/8	30.61	34.49	14.41	28.43	34.42	2.24
BN-based adaptive $L_p$	4/8	30.57	33.27	18.76	27.21	35.04	10.01
DetPTQ* (Ours)	4/8	<b>32.96</b>	<b>37.04</b>	<b>19.96</b>	<b>28.95</b>	<b>36.51</b>	<b>12.42</b>
MSE	4/4	27.75	29.10	8.04	24.81	30.31	2.74
Cosine	4/4	21.59	19.77	0.27	21.48	18.97	0.04
BN-based adaptive $L_p$	4/4	24.77	28.25	8.12	25.23	27.43	3.38
DetPTQ* (Ours)	4/4	<b>30.04</b>	<b>31.18</b>	<b>9.87</b>	<b>27.67</b>	<b>32.13</b>	<b>5.65</b>

Table 2: Comparison DetPTQ\* with the simple PTQ method optimized by various metrics on COCO. W/A means the bit which weight/activation is quantized to.

blocks before  $B_l$  have been quantized and the blocks after  $B_l$  are in floating-point.

As shown in Algorithm 1, the quantization process for a block includes two steps. The first step is to select the  $p$  value. Our experiments in Section 5.3 shows the quantization of weight is not sensitive to the selection of  $p$ . Therefore, we only use the scale factor for activation values to speedup the search of  $p$ . Given a set of values  $P = \{p_i \mid i = 1, 2, \dots, k\}$  for  $L_p$  metric, we can optimize the inner problem in Eq 14 to get a set of activation scale factors  $S = \{s_{p_i}^* \mid i = 1, 2, \dots, k\}$  by minimizing the given  $L_p$  metric. Because there are only a small number activation scale factors in a block, the  $p$  selection process executes quickly. The second step is to optimize to the quantization parameters for both activation and weight to minimize the local reconstruction loss using the selected  $p$  value. The output of the quantized block is used as the input of the next layer.

## 5. Experimental Results

To evaluate the effectiveness of our proposed DetPTQ, we experiment on the COCO [23] benchmark for 2D object detection and KITTI [9] benchmark for 3D object detection. We compare DetPTQ with the existing PTQ approaches on various CNN detectors, including RetinaNet [22], FasterRCNN [29] and PointPillar [18]. Performance of 2D detection is evaluated by standard COCO metrics with mean average precision (mAP) on the validation set. As to KITTI, we pick the standard metrics and report the 3D box and 2D bounding box results at AP40.

### 5.1. Implementation Details

All the FP models in our paper use open-source codes from MMDetection [3] and MMDetection3D [7]. For COCO, we randomly pick a total of 256 training samples with a shorter edge to 800/600 pixels for ResNet [12] / Mo-

bileNetV2 [30] as the calibration dataset. As to KITTI, the number of calibration samples is set to 128. Following the implementation previous work [20, 32], the head of the network keeps full-precision, the first and the last layer are quantized to 8 bits. We execute block reconstruction for backbone and layer reconstruction for neck, respectively. We execute all experiments on Nvidia Tesla V100 GPU.

The balancing hyper-parameter  $\alpha$  in Equation 10 is 0.1/0.001 for  $L_1$ /IOU in the exploration of ODOL. To obtain the FP **positive boxes** in ODOL, the score threshold  $\theta$  is 0.05 and the NMS threshold is 0.5. Given a  $p$  value for  $L_p$ , we optimize all activation scale factors in a block by Adam optimizer with the learning rate 3e-4, iterations 5000 in Algorithm 1 line 6. We also optimize the scaling factors of convolution layers which do not belong to any block using Adam optimizer. The setting of local quantization reconstruction (i.e., Algorithm 1 line 14) is kept the same with QDrop, except that the warmup of rounding loss is 0.4.

### 5.2. Comparison with other PTQ Methods

As described in Section 3, PTQ can be divided into simple PTQ and advanced PTQ by whether optimizing the rounding variable. Our method can be applied to both simple and advanced PTQ. We try our ODOL-based adaptive  $L_p$  metric on the simple PTQ method and denote it as DetPTQ\*, while we adopt DetPTQ in advanced PTQ to get higher quantization accuracy.

#### 5.2.1 Result on COCO Benchmark

For simple PTQ, we compare the standard methods that grid searches the quantization parameters by minimizing the MSE [26] and Cosine distance [33] between activations before and after quantization. We also compare a related work [27], which uses the variance information from BN [15] to define a BN-based  $L_p$  metric to conduct the local block-wise optimization. We denote this method as BN-based adaptive  $L_p$ .

We set  $P = \{1, 1.5, 2, 2.5, 3, 3.5, 4, 4.5\}$  in our experiments.

Method	Bits(W/A)	Faster RCNN			RetinaNet		
		ResNet-18	ResNet-50	MobileNetV2	ResNet-18	ResNet-50	MobileNetV2
FP	32/32	34.23	38.46	29.91	31.67	37.38	28.40
RAPQ [34]	4/4	31.17	32.76	20.96	29.03	33.72	21.76
AdaQuant [14]	4/4	32.89	35.03	22.77	30.34	35.84	22.27
AdaRound [25]	4/4	32.45	34.22	23.32	30.41	35.59	22.16
BRECQ [20]	4/4	32.47	34.31	23.76	30.42	35.71	22.23
QDROP [32]	4/4	33.13	36.98	25.04	30.54	36.13	25.71
DetPTQ (Ours)	4/4	<b>33.82</b>	<b>37.82</b>	<b>25.49</b>	<b>31.12</b>	<b>36.83</b>	<b>27.14</b>
AdaRound	3/3	29.97	32.94	18.56	27.88	32.36	15.87
BRECQ	3/3	30.12	33.32	19.02	28.07	32.84	17.02
QDROP	3/3	30.93	34.32	21.31	28.48	33.45	18.73
DetPTQ (Ours)	3/3	<b>32.11</b>	<b>34.97</b>	<b>21.94</b>	<b>29.30</b>	<b>34.48</b>	<b>19.40</b>
AdaRound	2/4	28.44	31.25	19.03	24.73	32.87	15.81
BRECQ	2/4	29.21	32.10	19.45	27.76	33.11	16.02
QDROP	2/4	30.68	34.41	<b>21.56</b>	28.51	33.52	18.62
DetPTQ (Ours)	2/4	<b>30.72</b>	<b>35.31</b>	21.31	<b>28.93</b>	<b>34.87</b>	<b>19.35</b>

Table 3: Comparison DetPTQ with various SOTA advanced PTQ methods on COCO.

Method	Bits(W/A)	PointPillar 3D-Box			PointPillar Bounding-Box		
		easy@AP40	moderate@AP40	hard@AP40	easy@AP40	moderate@AP40	hard@AP40
FP	32/32	76.72	64.48	60.79	84.05	75.44	72.58
BRECQ [20]	4/8	72.93	60.78	58.11	81.23	73.21	70.76
QDROP [32]	4/8	74.77	62.04	58.81	82.80	73.96	71.43
DetPTQ (Ours)	4/8	<b>76.02</b>	<b>63.89</b>	<b>59.92</b>	<b>83.45</b>	<b>74.66</b>	<b>72.04</b>
BRECQ	4/4	62.83	51.24	48.03	77.45	68.26	66.01
QDROP	4/4	64.42	52.63	49.68	79.51	70.52	67.06
DetPTQ (Ours)	4/4	<b>68.03</b>	<b>55.85</b>	<b>52.79</b>	<b>83.02</b>	<b>73.27</b>	<b>70.42</b>

Table 4: Comparison on PointPillar with various PTQ algorithms on KITTI.

According to the findings presented in Table 2, it is evident that the implementation of DetPTQ\* can lead to a substantial enhancement in the simple PTQ method. It should be noted that relying solely on local information may not always yield accurate results. For instance, MSE, Cosine and BN-based adaptive  $L_p$  obtain 27.75, 21.59 and 24.77 mAP on W4A4 Faster RCNN-ResNet18, while DetPTQ\* exhibits an improvement of 30.04 mAP for the simple PTQ method. Our DetPTQ\* demonstrates remarkable improvement in the performance across all networks and bitwidth settings. This outcome highlights the efficacy of utilizing global information from the performance loss to derive a better quantization performance.

We also compare our method with strong advanced baselines including AdaRound, BRECQ and QDROP. The results are shown in Table 3. With W4A4 quantization, we observe that DetPTQ achieves less than 1% mAP drop on

As certain models are unavailable, we present the results of other quantization methods utilizing their open-source codes with all FP models from MMDetection. It is possible that our values may differ from those reported in their papers.

the ResNet-based object detection networks. As for W3A3 quantization, the task becomes harder but our method can also achieve significant improvement. In the most difficult W2A4 setting, our method can still improve the performance of the model in most cases. For instance, DetPTQ achieves 1.42% mAP improvement on RetinaNet-ResNet50 compared to the baseline QDrop. Taking all experiments together, our method is orthogonal to the selection of simple and advanced PTQ as well as provides a convincing uplift on the object detection network.

### 5.2.2 Result on KITTI Benchmark

We choose PointPillar with SECOND backbone to evaluate the performance of DetPTQ on the KITTI benchmark for 3D object detection. For PointPillar, there is an additional head known as the direction prediction head. In addition to the localization offset, we decode the direction output to calculate the real coordinate, and then execute the localization loss ( $\mathcal{L}_{loc}$ ) to measure the coordinate distance of **positive boxes** between the FP and quantized outputs.

Model	Variable	Optimal $p$	#Params
Layer1.1.Conv2	$s_a$	3.5	2
	$s_a + V$	3.5	2+1152
Layer4.1.Conv2	$s_a$	1.5	2
	$s_a + V$	1.5	2+9216

Table 5: Ablation study for different quantization parameters. We only quantize one layer (Layer1.1.Conv2 or Layer4.1.Conv2) on RetinaNet-ResNet18 at W3A3. #Params refers to the number of parameters to optimize.

As Table 4 shows, the results of our DetPTQ are indeed close to FP model with negligible accuracy drop on PointPillar-SECOND detector. At W4A8, we achieve a decrease of less than 1% compared to FP accuracy for the first time. As for the challenging W4A4, our DetPTQ achieves 0.61%  $\sim$  3.61% improvement compared with strong baselines. For 3D box @AP40, we outperform QDrop by a large margin of 3.61%/3.22%/3.11% for easy/moderate/hard.

### 5.3. Ablation Study

#### 5.3.1 The Quantization Parameters in ODOL

We only set the activation scale factor ( $s_a$ ) as quantization parameters to optimize Eq 14 when given different  $p$  values, then select the lowest  $\mathcal{L}_{ODOL}$  and its corresponding  $p$  value. However, for advanced PTQ, there is another kind of weight parameter named the rounding variable ( $V$ ), which determines whether the weight values round up or down. As shown in Table 5, we experiment with optimizing  $s_a$  and  $V$  jointly as quantization parameters and find the optimal  $p$  value of  $L_p$  metric. The experiments show that  $V$  is not sensitive to the optimization of optimal  $p$  value. Introducing  $V$  to the optimization will greatly increase the optimizing time, so we do not consider  $V$ . As to the weight scale factors, we follow the implementation of Qdrop and BRECQ with the optimization by minimizing MSE distance.

#### 5.3.2 Effect of ODOL on Different Functions

To show the effectiveness of different functions for the Object Detection Output Loss, we quantize RetinaNet-ResnetNet18 and Faster RCNN-ResNet18 at W4A4 as examples to conduct the ablation study. Table 6 shows the experimental results. KL and  $L_2$  measure the distance between the quantized and FP feature map for the classification head. IOU loss measures the spatial difference of bounding boxes from quantized and FP output.  $L_1$  is leveraged for the difference of coordinate distance. We observe that choosing KL+ $L_1$  as ODOL yields the best quantization result among all metrics. Hence we finally set KL+ $L_1$  as the ODOL functions to represent the task information of

Model	Metric				mAP
	$L_2$	KL	$L_1$	IOU	
RetinaNet-ResNet18	✓		✓		31.07
	✓	✓	✓		<b>31.12</b>
		✓		✓	30.21
Faster RCNN-ResNet18			✓	✓	30.64
	✓		✓		33.41
	✓	✓	✓		<b>33.82</b>
			✓	✓	33.04
		✓	✓	33.11	

Table 6: Ablation study of different combination for ODOL. We mark a ✓ when adopt the loss function.

object detection to guide the optimization of the adaptive  $L_p$  metric.

KL divergence is widely used to measure the error of probability distribution. So it can better reflect the error of classification features than MSE. We also postulate that minimizing the difference of coordinate distance ( $L_1$ ) directly rather than spatial difference (IOU loss) can better represent localization error for PTQ.

#### 5.3.3 Comparison with other Metrics

To illustrate the superiority of our ODOL-based  $L_p$  metric for a broader comparison, we conduct further experiments to compare it with other metrics. In Table 7, we compare the adaptive BN-based  $L_p$  and local MSE with our ODOL-based  $L_p$  on the advanced PTQ method. Minimizing the distance of intermediate feature maps before and after quantization, those two metrics are denoted as the local metric. Our DetPTQ introduces the global performance loss information to determine the  $L_p$  metric. We can see that the ODOL-based adaptive  $L_p$  metric can improve the accuracy by 0.58% compared with the MSE at the W4A4 bit setting. The ODOL also outperforms the BN to guide the  $p$  value and improve by 2.36% on RetinaNet-ResNet18 compared with based on BN at W4A4.

Method	Metric	Bits(W/A)	
		W4A4	W3A3
Local	MSE	30.54	28.48
Local	BN-based adaptive $L_p$	28.76	27.16
<b>Global</b>	<b>ODOL-based adaptive <math>L_p</math></b>	<b>31.12</b>	<b>29.30</b>

Table 7: Results of the parameter optimization by different metrics on RetinaNet-ResNet18 at W4A4.

## 6. Conclusion

In this paper, we explored the application of post-training quantization on object detection networks. At first, we observed that the parameter  $p$  in  $L_p$  metric has a significant in-

fluence on quantization for object detection networks. And we indicated that it is necessary to set an adaptive  $L_p$  metric. To solve these problems, we propose the Object Detection Output Loss (ODOL) as an approximation of performance loss and then optimize the  $p$  value using ODOL as the reconstruction quantization loss. We proposed the framework, DetPTQ, which achieved the SOTA on networks for both 2D and 3D object detection tasks.

## References

- [1] Ron Banner, Yury Nahshan, and Daniel Soudry. Post training 4-bit quantization of convolutional networks for rapid-deployment. *Advances in Neural Information Processing Systems*, 32, 2019. **3**
- [2] Yoshua Bengio, Nicholas Léonard, and Aaron Courville. Estimating or propagating gradients through stochastic neurons for conditional computation. *arXiv preprint arXiv:1308.3432*, 2013. **3**
- [3] Kai Chen, Jiaqi Wang, Jiangmiao Pang, Yuhang Cao, Yu Xiong, Xiaoxiao Li, Shuyang Sun, Wansen Feng, Ziwei Liu, Jiarui Xu, Zheng Zhang, Dazhi Cheng, Chenchen Zhu, Tianheng Cheng, Qijie Zhao, Buyu Li, Xin Lu, Rui Zhu, Yue Wu, Jifeng Dai, Jingdong Wang, Jianping Shi, Wanli Ouyang, Chen Change Loy, and Dahua Lin. MMDetection: Open mmlab detection toolbox and benchmark. *arXiv preprint arXiv:1906.07155*, 2019. **6**
- [4] Peng Chen, Jing Liu, Bohan Zhuang, Minghui Tan, and Chunhua Shen. Aq: Towards accurate quantized object detection. In *Proceedings of the IEEE/CVF Conference on Computer Vision and Pattern Recognition*, pages 104–113, 2021. **3**
- [5] Jungwook Choi, Zhuo Wang, Swagath Venkataramani, Pierce I-Jen Chuang, Vijayalakshmi Srinivasan, and Kailash Gopalakrishnan. Pact: Parameterized clipping activation for quantized neural networks. *arXiv preprint arXiv:1805.06085*, 2018. **2**
- [6] Yoni Choukroun, Eli Kravchik, Fan Yang, and Pavel Kisilev. Low-bit quantization of neural networks for efficient inference. In *2019 IEEE/CVF International Conference on Computer Vision Workshop (ICCVW)*, pages 3009–3018. IEEE, 2019. **3**
- [7] MMDetection3D Contributors. MMDetection3D: Open-MMLab next-generation platform for general 3D object detection. <https://github.com/open-mmlab/mmdetection3d>, 2020. **6**
- [8] Steven K Esser, Jeffrey L McKinstry, Deepika Bablani, Rathinakumar Appuswamy, and Dharmendra S Modha. Learned step size quantization. *arXiv preprint arXiv:1902.08153*, 2019. **1, 2**
- [9] Andreas Geiger, Philip Lenz, Christoph Stiller, and Raquel Urtasun. Vision meets robotics: The kitti dataset. *International Journal of Robotics Research (IJRR)*, 2013. **6**
- [10] Amir Gholami, Sehoon Kim, Zhen Dong, Zhewei Yao, Michael W Mahoney, and Kurt Keutzer. A survey of quantization methods for efficient neural network inference. *arXiv preprint arXiv:2103.13630*, 2021. **1**
- [11] Jianping Gou, Baosheng Yu, Stephen J Maybank, and Dacheng Tao. Knowledge distillation: A survey. *International Journal of Computer Vision*, 129(6):1789–1819, 2021. **1**
- [12] Kaiming He, Xiangyu Zhang, Shaoqing Ren, and Jian Sun. Deep residual learning for image recognition. In *Proceedings of the IEEE conference on computer vision and pattern recognition*, pages 770–778, 2016. **6**
- [13] Yihui He, Xiangyu Zhang, and Jian Sun. Channel pruning for accelerating very deep neural networks. In *Proceedings of the IEEE international conference on computer vision*, pages 1389–1397, 2017. **1**
- [14] Itay Hubara, Yury Nahshan, Yair Hanani, Ron Banner, and Daniel Soudry. Accurate post training quantization with small calibration sets. In *International Conference on Machine Learning*, pages 4466–4475. PMLR, 2021. **3, 7**
- [15] Sergey Ioffe and Christian Szegedy. Batch normalization: Accelerating deep network training by reducing internal covariate shift. In *International conference on machine learning*, pages 448–456. PMLR, 2015. **3, 6**
- [16] Benoit Jacob, Skirmantas Kligys, Bo Chen, Menglong Zhu, Matthew Tang, Andrew Howard, Hartwig Adam, and Dmitry Kalenichenko. Quantization and training of neural networks for efficient integer-arithmetic-only inference. In *Proceedings of the IEEE conference on computer vision and pattern recognition*, pages 2704–2713, 2018. **3**
- [17] Raghuraman Krishnamoorthi. Quantizing deep convolutional networks for efficient inference: A whitepaper. *arXiv preprint arXiv:1806.08342*, 2018. **2**
- [18] Alex H. Lang, Sourabh Vora, Holger Caesar, Lubing Zhou, Jiong Yang, and Oscar Beijbom. Pointpillars: Fast encoders for object detection from point clouds. In *Proceedings of the IEEE/CVF Conference on Computer Vision and Pattern Recognition (CVPR)*, June 2019. **2, 6**
- [19] Rundong Li, Yan Wang, Feng Liang, Hongwei Qin, Junjie Yan, and Rui Fan. Fully quantized network for object detection. In *Proceedings of the IEEE/CVF Conference on Computer Vision and Pattern Recognition*, pages 2810–2819, 2019. **3**
- [20] Yuhang Li, Ruihao Gong, Xu Tan, Yang Yang, Peng Hu, Qi Zhang, Fengwei Yu, Wei Wang, and Shi Gu. Brcq: Pushing the limit of post-training quantization by block reconstruction. *arXiv preprint arXiv:2102.05426*, 2021. **2, 3, 6, 7**
- [21] Tsung-Yi Lin, Piotr Dollár, Ross Girshick, Kaiming He, Bharath Hariharan, and Serge Belongie. Feature pyramid networks for object detection. In *Proceedings of the IEEE conference on computer vision and pattern recognition*, pages 2117–2125, 2017. **3**
- [22] Tsung-Yi Lin, Priya Goyal, Ross Girshick, Kaiming He, and Piotr Dollár. Focal loss for dense object detection. In *Proceedings of the IEEE international conference on computer vision*, pages 2980–2988, 2017. **1, 2, 3, 6**
- [23] Tsung-Yi Lin, Michael Maire, Serge Belongie, James Hays, Pietro Perona, Deva Ramanan, Piotr Dollár, and C Lawrence Zitnick. Microsoft coco: Common objects in context. In *European conference on computer vision*, pages 740–755. Springer, 2014. **1, 3, 6**

- [24] Jiawei Liu, Lin Niu, Zhihang Yuan, Dawei Yang, Xinggong Wang, and Wenyu Liu. Pd-quant: Post-training quantization based on prediction difference metric. *arXiv preprint arXiv:2212.07048*, 2022. [3](#), [5](#)
- [25] Markus Nagel, Rana Ali Amjad, Mart Van Baalen, Christos Louizos, and Tijmen Blankevoort. Up or down? adaptive rounding for post-training quantization. In *International Conference on Machine Learning*, pages 7197–7206. PMLR, 2020. [1](#), [2](#), [3](#), [7](#)
- [26] Markus Nagel, Marios Fournarakis, Rana Ali Amjad, Yelysei Bondarenko, Mart Van Baalen, and Tijmen Blankevoort. A white paper on neural network quantization. *arXiv preprint arXiv:2106.08295*, 2021. [6](#)
- [27] Yury Nahshan, Brian Chmiel, Chaim Baskin, Evgenii Zheltonozhskii, Ron Banner, Alex M Bronstein, and Avi Mendelson. Loss aware post-training quantization. *Machine Learning*, 110(11):3245–3262, 2021. [3](#), [6](#)
- [28] Alexander Neubeck and Luc Van Gool. Efficient non-maximum suppression. In *18th International Conference on Pattern Recognition (ICPR'06)*, volume 3, pages 850–855. IEEE, 2006. [5](#)
- [29] Shaoqing Ren, Kaiming He, Ross Girshick, and Jian Sun. Faster r-cnn: Towards real-time object detection with region proposal networks. *Advances in neural information processing systems*, 28, 2015. [1](#), [2](#), [3](#), [6](#)
- [30] Mark Sandler, Andrew Howard, Menglong Zhu, Andrey Zhmoginov, and Liang-Chieh Chen. Mobilenetv2: Inverted residuals and linear bottlenecks. In *Proceedings of the IEEE conference on computer vision and pattern recognition*, pages 4510–4520, 2018. [6](#)
- [31] Changbao Wang, DanDan Zheng, Yuanliu Liu, and Liang Li. Leveraging inter-layer dependency for post-training quantization. In *Advances in Neural Information Processing Systems*. [5](#)
- [32] Xiuying Wei, Ruihao Gong, Yuhang Li, Xianglong Liu, and Fengwei Yu. Qdrop: Randomly dropping quantization for extremely low-bit post-training quantization. *arXiv preprint arXiv:2203.05740*, 2022. [2](#), [3](#), [6](#), [7](#)
- [33] Di Wu, Qi Tang, Yongle Zhao, Ming Zhang, Ying Fu, and Debing Zhang. Easyquant: Post-training quantization via scale optimization. *arXiv preprint arXiv:2006.16669*, 2020. [3](#), [6](#)
- [34] Hongyi Yao, Pu Li, Jian Cao, Xiangcheng Liu, Chenying Xie, and Bingzhang Wang. Rapq: Rescuing accuracy for power-of-two low-bit post-training quantization. *arXiv preprint arXiv:2204.12322*, 2022. [3](#), [7](#)
- [35] Jiahui Yu, Yuning Jiang, Zhangyang Wang, Zhimin Cao, and Thomas Huang. Unitbox: An advanced object detection network. In *Proceedings of the 24th ACM international conference on Multimedia*, pages 516–520, 2016. [5](#)
- [36] Zhihang Yuan, Chenhao Xue, Yiqi Chen, Qiang Wu, and Guangyu Sun. Ptq4vit: Post-training quantization for vision transformers with twin uniform quantization. In *European Conference on Computer Vision*, pages 191–207. Springer, 2022. [3](#)